PERGAMON

Chemical Engineering Science 55 (2000) 3729–3738

Chemical Engineering Science

Steady-state simulation of a continuous moving bed reactor in the pulp and paper industry

Natércia C.P. Fernandes, José A.A.M. Castro*

Department of Chemical Engineering, University of Coimbra, 3030 Coimbra, Portugal

Received 4 June 1999; accepted 24 November 1999

Abstract

This paper is concerned with the mathematical modeling and simulation of the steady-state operation of an industrial moving bed heterogeneous reactor for the kraft pulping of *Eucalyptus globulus*. The cooking takes place in a single-vessel hydraulic digester adapted for isothermal cooking (ITC), a further development of the modified continuous cooking (MCC) process. A heterogeneous model is used to take into account the different phases, each with distinct profiles of temperature and concentration of organic (lignin, cellulose and hemicellulose) and inorganic (effective alkali and sulfide) compounds. The numerical solution of the model is based on a non-uniform discretization strategy to cope with special geometric and operational features of the digester. The decrease in bulk porosity caused by the compaction of the bed and the progressive increase in the voidage of chips as a result of chemical reactions are incorporated into the model as well as the resulting implications in the entrapped and free liquor flows. The model presented here can be used in optimization studies and has been validated with data from an industrial mill.

Keywords: Simulation; Mathematical modeling; Multi-phase reactor; Moving bed; Pulping digester; Isothermal cooking

1. Introduction

The pulp and paper industry plays a very important role in the world and particularly in the European economies. In order to optimize its performance and improve the quality of the pulp, this industry has a real need for tools that enable the simulation of experiments that cannot be afforded or that might be risky in a real industrial context. The most critical piece of equipment in a Kraft pulp and paper plant is the digester, known as the heart of the mill. It is a very special and complex heterogeneous reactor where a moving bed of wood chips contacts and reacts with sodium hydroxide and sodium sulfide in a liquid phase (Kraft process), in order to dissolve lignin and therefore to release the fibers of cellulose. Since the chips are porous and are soaked with liquor, the digester is a reactor with three simultaneous phases, whose behavior is strongly dependent on the heat and mass transfer phenomena and on the rate of chemical reactions of all wood components.

The need for predicting the behavior of such reactor has been the driving force for much research work on digester modeling over the past decades. A pioneer effort was made by Vroom (1957), who developed the concept of "H-factor", still in use presently. Temperature and cooking time for batch digesters were lumped into a single variable, easing the task of choosing a pair of operational values for those variables, in order to achieve a certain extent of cooking. Many other empirical models of the type of the H-factor model have been developed since then. Simultaneously, a wide range of physically based models has also been proposed. The main differences among such models lie in the number of phases considered, the number of species in each phase, the kinetic rate equations, the type of digester and the degree of accuracy in updating some intermediate variables as the reactions proceed (Grace & Malcolm, 1989).

Any critical review of physically based models for Kraft pulping digesters must include the work of Johnsson (1970). He is responsible for the development of the earliest dynamic model, although its solution was obtained with a steady-state version of the equations. His

* Corresponding author. Tel.: +351-39-798700; fax: +351-39-798703.

E-mail addresses: natercia@eq.uc.pt (N. C. P. Fernandes), eq1jmc@eq.uc.pt (J. A. A. M. Castro).

0009-2509/00/$ - see front matter
PII: S0009-2509(00)00063-4

work was later followed by that of Smith and Williams (1974), who included a kinetic model, often designated as the Purdue model, in the reactor equations. It considers the wood matrix (solid phase) as made of five species that react with the inorganic chemicals dissolved in the liquid. The digester was approximated by a series of continuous stirred-tank reactors (CSTRs) and this approach was continued by other researchers, namely Christensen, Albright and Williams (1982) and Wisnewski, Doyle III and Kayihan (1997). They consider different concentrations in the entrapped and free liquors and update some variables according to the reaction extent.

Another notable contribution to Kraft delignification kinetics was presented by Gustafson, Shelder, McKean and Finlayson (1983) who proposed three separate reaction laws to characterize the rates of reaction of softwoods and assumed that wood is simply made of two main compounds. Later, Pu (1991) extended this work considering different equations for the degradation of cellulose and hemicellulose. Nóbrega and Castro (1997) adopted a similar conceptual model based on experimental data for *Eucalyptus globulus*, a hardwood that is a very important supply of short fiber for offset and printing paper. The delignification kinetics of this raw material was also investigated by Santos, Rodríguez, Gilarranz Moreno and García-Ochoa (1997) and Giudici and Park (1996).

With respect to the description of the fluid behavior inside the digester, the first contribution is due to Härkönen (1987). Using momentum balances coupled with heat and mass conservation equations, this researcher derived a steady-state model to simulate the operation of the digester. The column of chips was assumed orthotropic and the equations of the model were solved in both axial and radial directions. However, his approach does not discriminate between the entrapped liquid and the solid matrix of the wood and is based only on transfer phenomena, lacking any description of the chemical reactions involved in the pulping process. Later, Michelsen (1995) extended this work to describe the dynamic behavior of the reactor although such a model is only valid for Kappa numbers between 50 and 150 (Wisnewski et al., 1997) as a result of unrealistic simplifications in the kinetic model.

In the heterogeneous modeling approach adopted in this study the digester is basically represented as a series of mixing cells, where three different phases coexist and interact. With regard to previous works, the following points should be enlightened: (a) the digester under investigation is an industrial hydraulic reactor with isothermal cooking, a further development of modified continuous cooking (MCC); (b) the voidage of the chips is updated according to the extent of reaction but retaining the usual mass basis to define the solid concentrations; (c) the numerical solution of the model is based on a non-uniform discretization procedure that better takes into account the geometry of the system; (d) the radial displacement of liquid at the concurrent re-circulations is modeled by a more realistic strategy; (e) the axial variation in the compaction of the bed is accounted for with data provided by the mill and (f) industrially important variables such as total solids content (organic + inorganic) and final pulp consistency are also predicted.

2. Modeling

Fig. 1 shows a simplified representation of the continuous Kamyr digester with isothermal cooking whose steady-state operation is under investigation in this study. The high complexity of the reactor is mainly due to its unusual mechanical arrangements and to the very special features of its nearly isothermal operation. These include simultaneous concurrent and counter-current flows, multiple feeds, multiple liquid outputs and intermediate external heating points.

The digester is roughly a cylindric vessel in a vertical position and, in its upper part, the solid and the free liquid phases flow downwards concurrently while, in the lower part, the free liquor flows upwards counter-currently with the chips. Moreover, at several levels of the digester's height the wall is built as a set of screens that enable the withdrawal of free liquor from the moving bed of chips. The resulting outlet liquor streams, extracted at such positions, are most often enriched by a fresh cooking liquor feed and further heated up in a heat exchanger

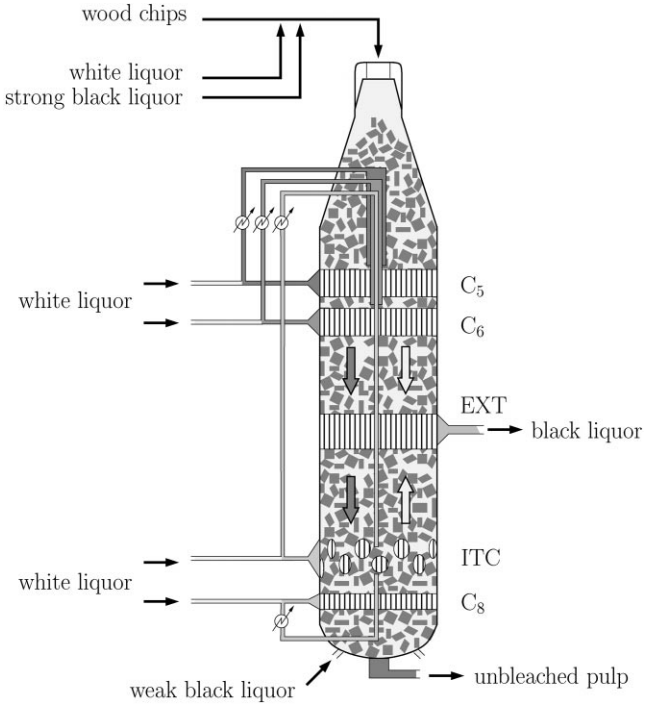

Fig. 1. Simplified schematic representation of the digester with isothermal cooking.

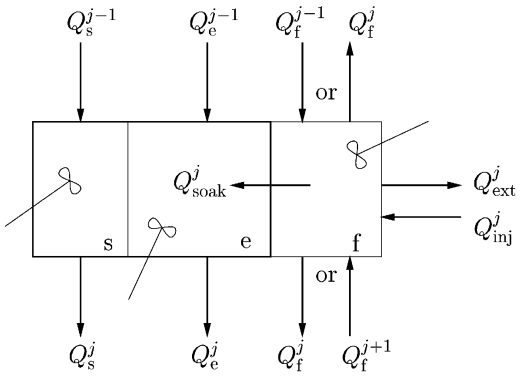

Fig. 2. Representation of a generic cell (j). s stands for solid matrix, e for entrapped liquor and f for free liquor.

before being injected back into the digester at a similar axial location. To describe the reactor, a cell model approach similar to that initially proposed by Smith and Williams (1974) is also adopted here. Each cell is characterized by three different phases and by 15 dependent variables representing concentrations and temperatures. Fig. 2 illustrates such compartment unit for a general cell j.

The amount of organic material in the solid phase depends only on the extent of the chemical reactions taking place within the chip and then it can be described by

$$0 = Q_c I_s^{j-1} - Q_c I_s^j + (1-\varepsilon_d) V_{cell} r_I \quad \text{with } I = L, C, H \tag{1}$$

where L_s, C_s and H_s represent the concentrations (mass fraction, based on the initial oven dry wood) of lignin, cellulose and hemicellulose in the solid phase, respectively. For calculating the different reaction rates, r_I, the kinetic equations proposed by Nóbrega and Castro (1997) for *E. globulus* (Appendix) are employed. The inorganic chemicals in the entrapped liquor attack the solid phase and dissolve the organic compounds of the wood into this liquor. Simultaneously, mass transfer of these species also take place between the entrapped and the free liquors. Thus, the mass balance equations for the entrapped liquor are

$$0 = Q_e^{j-1} I_e^{j-1} - Q_e^j I_e^j + Q_{soak}^j I_f^j + k_{m_I} V_{cell}(1-\varepsilon_d)(I_f^j - I_e^j) - (1-\varepsilon_d)\rho_{c_{OD}} V_{cell} r_I \quad \text{with } I = L, C, H, \tag{2}$$

$$0 = Q_e^{j-1} E_e^{j-1} - Q_e^j E_e^j + Q_{soak}^j E_f^j + k_{m_E} V_{cell}(1-\varepsilon_d)(E_f^j - E_e^j) - (1-\varepsilon_d)\varepsilon_c V_{cell} r_E, \tag{3}$$

$$0 = Q_e^{j-1} S_e^{j-1} - Q_e^j S_e^j + Q_{soak}^j S_f^j + k_{m_S} V_{cell}(1-\varepsilon_d)(S_f^j - S_e^j), \tag{4}$$

where E_e^j and S_e^j represent the concentrations of effective alkali and sodium sulfide in the entrapped liquid in the cell j. In the free liquor, though, there is no chemical reaction and thus the mass balances are simply governed by mass transfer phenomena, in particular by convection and diffusion between the two liquid phases

$$0 = Q_f^{j\pm1} I_f^{j\pm1} - (Q_{ext}^j + Q_{soak}^j + Q_f^j) I_f^j + Q_{inj}^j I_{inj}^j + k_{m_I} V_{cell}(1-\varepsilon_d)(I_e^j - I_f^j) \quad \text{with } I = L, C, H, E, S. \tag{5}$$

Since the heat effects due to chemical reaction inside the chips are very moderate, the solid matrix and the entrapped liquor are assumed to be at the same temperature. However, because of the sharp changes in temperature imposed at several axial positions, i.e., in the extraction lines, different energy balances are written for the free liquor and for the chips (solid matrix + entrapped liquor) in order to determine the temperature profiles along the reactor

$$0 = Q_f^{j\pm1}(\rho C_p)_f^{j\pm1} T_f^{j\pm1} - (Q_{ext}^j + Q_{soak}^j + Q_f^j) \times (\rho C_p)_f^j T_f^j + Q_{inj}^j (\rho C_p)_{inj}^j T_{inj}^j + k_h V_{cell}(1-\varepsilon_d)(T_c^j - T_f^j), \tag{6}$$

$$0 = Q_c(\rho C_p)_c^{j-1} T_c^{j-1} - Q_c(\rho C_p)_c^j T_c^j + Q_{soak}^j (\rho C_p)_f^j T_f^j + k_h V_{cell}(1-\varepsilon_d)(T_f^j - T_c^j) + (1-\varepsilon_d)\rho_{c_{OD}} \sum_I (-\Delta H_R) r_I \quad \text{with } I = L, C, H. \tag{7}$$

In Eqs. (5) and (6) the superscript $j+1$ is employed in the counter-current part while $j-1$ is used in the concurrent zone. All liquid and solid flows, as well as their main properties, are updated along the digester since they depend on the extent of the reactions and on the compaction of the bed. In fact, as the reactions proceed, the voidage of the chip increases due to the dissolution of the organic material. Wisnewski and Doyle III (1996) and Wisnewski et al. (1997) claimed that, through a redefinition of mass concentrations, it could be possible to overtake some necessary assumptions in earlier Purdue models, namely in calculating the chip porosity. However, this step ahead can be achieved without the inconvenience of having to change the usual industrial basis (mass of wood component per mass of initial oven dry chip)

$$\varepsilon_c = 1 - \eta(1-\varepsilon_{c,i}), \tag{8}$$

where the yield η is given by the sum of the mass fractions of the three components of wood

$$\eta = L_s + C_s + H_s. \tag{9}$$

The thermal capacity of the chips is calculated taking into account the relative amounts of solid material and of entrapped liquid at each axial position of the digester. Since the porosity changes during cooking, the flows

of the three phases vary too and the entrapped liquor volumetric flow is simply given by

$$Q_e = \varepsilon_c Q_c. \tag{10}$$

The free liquor volumetric flow rate decreases as much as the entrapped liquid flow increases, besides the abrupt changes in the free liquor flow at the injection and extraction points. While the chip's void fraction increases along the digester because of chemical reaction, the bed porosity decreases due to the progressive compaction of the packing. The so-called compaction factor is often defined as the ratio between the volume of a chip bulk outside the digester and the volume of the same amount of chips when placed inside the digester. Based on this definition, the porosity of the bed is given as a function of the compaction factor

$$\varepsilon_d = 1 - f(1 - \varepsilon_{pile}). \tag{11}$$

The void fraction of the chips outside the digester (ε_{pile}) is constant, but the compaction factor, f, in the digester is assumed in this study to decrease linearly along the reactor height, except near the bottom where it is constant; this assumption is based on the information provided by Kvaerner Pulping, the manufacturer of the digester and by the mill. In the present work, it has been approximated by the following equation:

$$f = \begin{cases} 0.032z + 1.01 & z < 35.9, \\ 2.16 & z \geqslant 35.9. \end{cases} \tag{12}$$

This variable also affects the residence time of wood particles inside the reactor because, as it increases, the downward movement of chips becomes slower. The interstitial velocities of the free liquor and of the moving bed of chips should, thus, be updated according to

$$u_f = \frac{Q_f}{\varepsilon_d A_d} \tag{13}$$

and

$$u_c = \frac{Q_c}{(1 - \varepsilon_d) A_d}. \tag{14}$$

In this study, other industrially important variables such as Kappa number, total solids content, yield and pulp consistency are also computed from the state variables characterized in Eqs. (1)–(7).

In the bottom half of the digester, the total circulation flows typical of an ITC cooking are higher than in the case of the conventional process, in order to attain smooth temperature and alkali profiles over the digester cross section. However, this raises mathematical difficulties in the numerical solution of the problem, since the discontinuities in the axial profiles of the main state variables become larger in these areas. This is especially important in the counter-current part, where the system model equations are of the boundary value type, thus requiring an iterative procedure for the solution of the corresponding non-linear set of equations. The numerical scheme adopted here is based on a nonuniform grid with the purpose of coping with such strong and sharp changes in the process variables characterizing the free liquor in the circulation zones as well as in the main extraction. An important advantage of this modeling strategy is that it allows to take into account the special features of each circulation of an industrial digester. In fact, distinct approaches were chosen for describing the effect of different circulations, based on the local geometrical arrangements and flow patterns (con- or counter-current). As illustrated in Fig. 3, the mixing cell concept is not used in the reactor zones corresponding to the upper circulation lines C_5 and C_6. The free liquor flowing from above the screens, Q_f, is assumed to follow an outwards conical flow path that leads it towards the screens plate. It is worth mentioning that this is the result of two main factors: the first is due to the pressure drop induced by the circulation pump and the second is concerned with the inner conical flow path of the liquid stream re-entering the digester with a very high flow rate, $Q_{ext} + Q_w$. This conical shape of the flow is generated by special flaps located at the outlets of the re-circulation pipe and also by the fact that the circulation flow rate, Q_{ext}, is much higher than Q_f. Such conical stream, thus, displaces the liquid flowing from above into the direction of the screen openings, before being also partially pumped out through the screens. These streams, of different concentrations and temperatures, are mixed in the circulation pump and the net result of this complex arrangement is the complete withdrawal of the liquid flowing with the chips at the top of this section of the reactor thus increasing its temperature and concentration (see also Fig. 1).

In opposition to this situation, the liquid injected in ITC and in C_8 circulations is assumed to mix completely with the ascendant liquid within the reactor. This is due

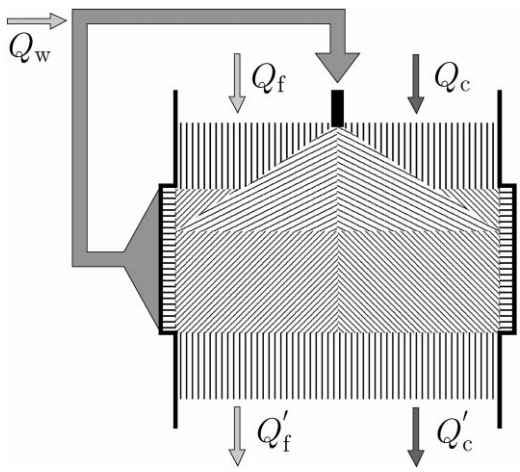

Fig. 3. Schematic representation of the re-circulations of the concurrent zone.

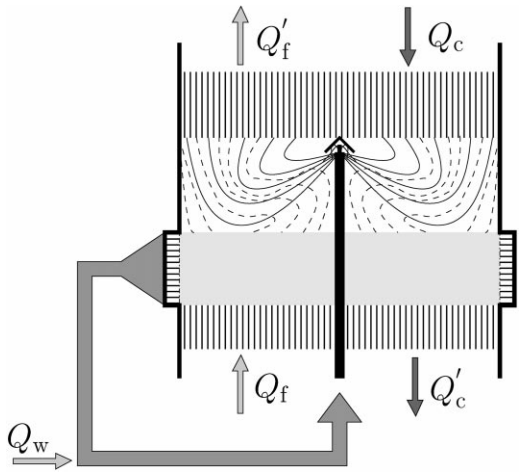

Fig. 4. Schematic representation of the re-circulation C_8 (counter-current zone).

to the special geometry of the inner re-circulation pipes and screens (see Fig. 4) and thus, these zones are modeled by means of the mixing cell approach, described before. C_8 is the only circulation of the digester where the recirculation flow is injected in an upwards direction. But, as Fig. 4 shows, this flow finds, right at the end of its inlet pipe, an inverted metal cone. Due to this mechanical arrangement, the liquid direction inverts according to the cone shape and is pushed downwards. Simultaneously, there is a significant flow of liquid with an upwards movement, imposed by the flow injected at the bottom of the digester. As a result of these strong and opposite forces, it seems reasonable to assume complete mixing, thus justifying the use of a single mixing cell in this position.

Finally, the zones without screens were split into several cells to guarantee that each cell height was small enough relative to the digester height. In particular, this procedure takes implicitly into account the positions of the screens and the size of the cells are also defined so that a given cell cannot belong simultaneously to parts with and without wall screens.

In the concurrent zone, since the differential problem is of initial value type, the step size used in the integration of the model equations is small (≈ 0.1 m) and is adapted in order to ensure that the axial variable matches the exact location of the screens and the injection points. In the counter-current part the model constitutes a boundary value problem and its solution is achieved by the use of a mixing cell approach and the simultaneous solution of all the resulting equations. This part has about 18 m and was divided into 25 cells. The size chosen for each cell has been investigated in order to minimize the cost of the numerical algorithm while ensuring the quality of the solution. This size is not uniform and takes into account the nature and the intensity of the phenomena taking place along this bottom part of the reactor. The cells, thus, have different heights and their size was distributed so that more cells appear between C_8 and the base of the digester where the state variables, especially temperature, exhibit steeper profiles.

3. Discussion of results

Temperature is undoubtedly one of the most important variables in the process of industrial cooking since it exerts a strong effect on the kinetics of both delignification and carbohydrate degradation. In the so-called isothermal cooking (ITC) this is used to take advantage of such strong but distinct dependencies by extending pulping for a period of time that is longer than in conventional cooking. Therefore, with ITC, the maximum temperature in the reactor is often lower, leading to a longer but smoother cooking. Fig. 5 illustrates typical temperature profiles along the reactor where strong discontinuities can be seen in the temperature of the free liquor phase, corresponding to the main re-circulation lines C_5 and C_6 where extraction, heating and injection back into the digester is carried out. Moreover, since the temperature levels below the main extraction screens are clearly higher than in conventional cooking the reaction is pushed further down the reactor, although at a slower rate than in the upper part. In the counter-current zone, where washing also occurs, the alkali concentration is kept above a minimum level by injecting fresh white liquor near the bottom of the digester (ITC), as shown in Fig. 6.

Once a convenient cooking temperature profile is imposed along the reactor, there is a need for an adequate alkali distribution policy to ensure high delignification rates for the process while maintaining the carbohydrate degradation at a minimum. Alkali is introduced through a white liquor multi-feed network, whose main branch reaches the digester right at its top (Fig. 6). The remaining white liquor is added to the circulations C_5 and

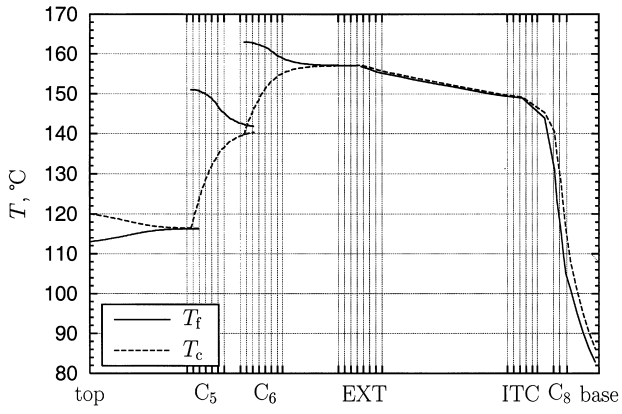

Fig. 5. Temperature of chips and free liquor.

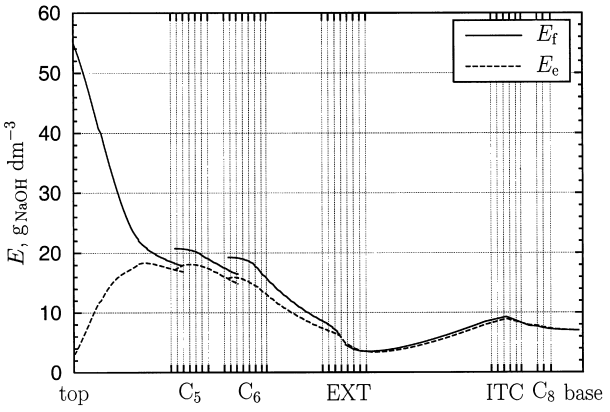

Fig. 6. Effective alkali in free and entrapped liquors.

C_6 and also to the bottom part of the reactor (ITC and C_8). At the top of the digester and just before the main white liquor feed the chips are often assumed to be completely filled with liquid that is basically constituted by water. This is a result of the original moisture in the wood and of the steam condensed within its porous structure in the steaming vessel. However, typical industrial scenarios for *Eucalyptus globulus* show that a small fraction of the chip is not fully soaked with water just before the high-pressure feeder. Thus, complete filling of the chips can only be achieved by penetration of a mixture of white and weak black liquors when it contacts the wood particles in the high pressure circulation line. This is why the effective alkali of the entrapped liquor (E_e) in Fig. 6 is different from zero at the top of the digester. The same applies to the sulfide ion as shown in Fig. 7.

In previous papers, the concentration of hydrogen sulfide is often assumed constant along the digester and is also considered as equal to the feed composition. Both assumptions are clearly unrealistic for *Eucalyptus globulus* (Magalhães et al., 1998) and thus are discarded in this work, as also advocated by Wisnewski et al. (1997). As can be seen in Fig. 7, both free and entrapped liquor concentrations change sharply in the first meters of the reactor and achieve a value in the main reaction zone that is markedly different from that at the entrance, as it happens in a real cooking. It is worth mentioning that the kinetics used here does not include any consumption of the sulfide ion, although its concentration in the entrapped liquor affects the rate of delignification in the solid (Appendix). The profiles shown in Fig. 7 are, therefore, the result of simple mass transfer phenomena between the entrapped and free liquors. In the concurrent zone the sulfide is gradually transferred from the free liquor to the chips while, in the counter-current part of the digester, the transfer occurs in the opposite direction. The values used for the heat and mass transfer coefficients in the counter-current zone are higher than in the concurrent zone due to the much higher relative interstitial velocity of the free liquor phase with respect to the wood chips. This is confirmed in Fig. 8, where strong discontinuities in the free liquor superficial velocity are also highlighted for the main circulations simulated in this study. An utmost important industrial variable is the final yield of the operation due to the high costs of the wood raw material. As illustrated in Fig. 9, the more extensive attack to the wood components occurs in the upper circulation zones (C_5 and C_6), as a result of simultaneous high values for temperature and effective alkali concentration (see also Figs. 5 and 6). Although this profile is frequently connected to the rate of delignification along the reactor height, significant amounts of carbohydrate are also degraded and removed from the wood matrix leading to a lower pulp quality.

In opposition to other definitions of dissolved solids (Wisnewski et al., 1997) that cannot be used for model validation with industrial data and do not follow the TAPPI procedure, in this work the total solids content ($\mathscr{S}$) in a cooking liquor represents both the organic and inorganic compounds in solution. This is an important industrial variable, particularly at the main extraction (EXT) due to its role in the heat and chemical recovery

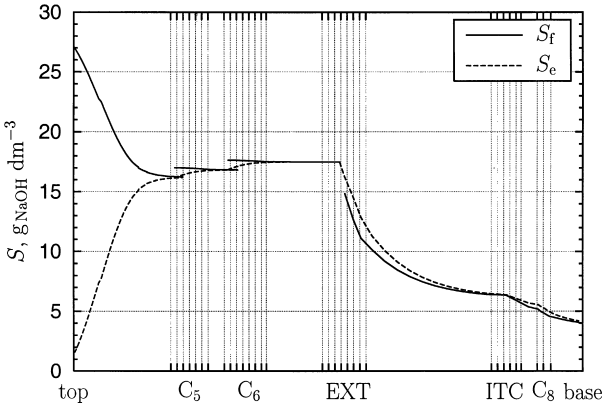

Fig. 7. Sulfide concentration in the entrapped and free liquors.

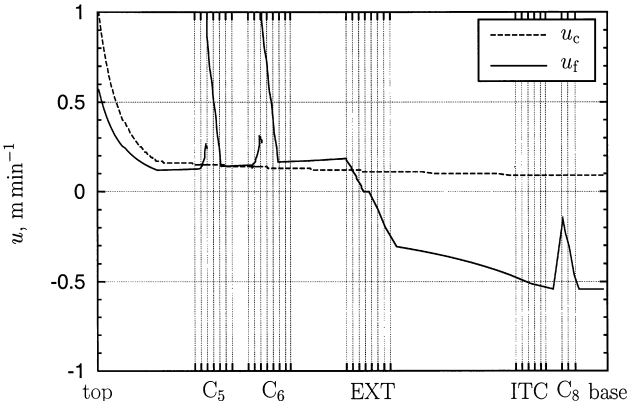

Fig. 8. Superficial velocities of the chips and the free liquor.

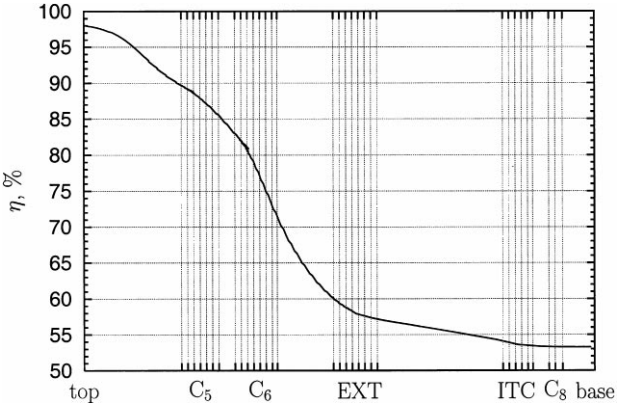

Fig. 9. Yield axial profile.

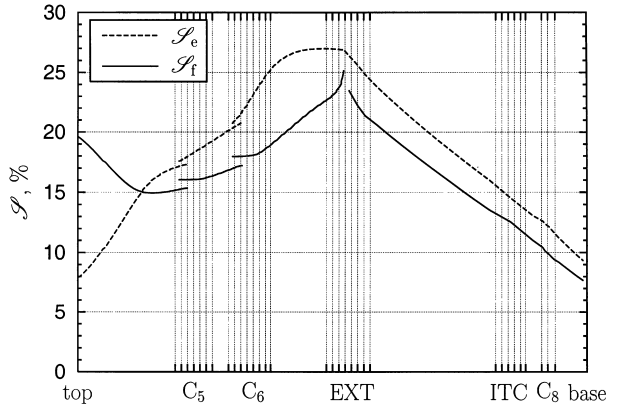

Fig. 10. Total solids content in the entrapped (e) and free (f) liquors.

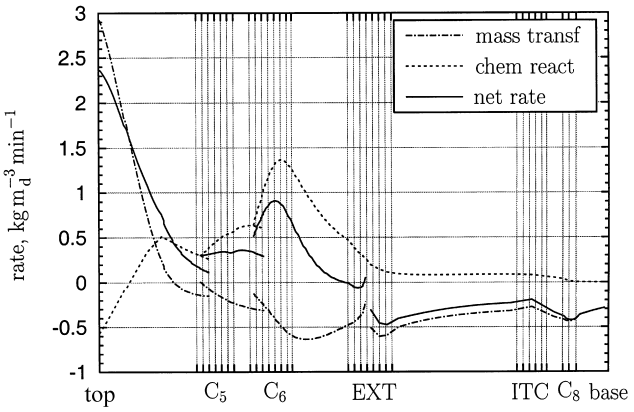

Fig. 11. Axial profiles of net mass transfer and of chemical reaction rates.

plants of the pulp mill. Moreover, it is invaluable for assessing the model ability to describe the behavior of the industrial digester as there are at least five circulations where it is possible to take samples of the liquor. There is an injection of strong black liquor at the top of the digester, which, together with the main feed of white liquor, ends up in a stream with a relatively high total solids content (see Fig. 10). The evolution of this variable in the free liquid depends only on the net rate of mass transfer of organic and inorganic materials between the two liquid phases. However, in the entrapped liquor it also depends on the rates of chemical reactions taking place in the porous chips. These two different contributions are represented separately in Fig. 11, in order to enable a better understanding of the total solids content profiles along the digester.

At the beginning, the net mass transfer from the surrounding liquid into the chips is positive (Fig. 11, dot–dashed line), thus giving rise to the initial decrease in the total solids content of the free liquor as shown in Fig. 10 (solid line). At this point, this mass transfer rate into the chips, which is high at the top of the digester, decreases and becomes negative (Fig. 11), meaning that it now occurs in the opposite direction, i.e., from the entrapped to the free liquor. Therefore, the solids content in the free liquid begins to increase (Fig. 10) exhibiting a minimum at the point where the net mass transfer vanishes (Fig. 11). Since then and until the end of the digester, the mass transfer into the chips is always negative, that is, it always occurs from the chips to the free liquor. This explains the increasing profile of solids content in the free liquid in the remaining concurrent part and the decreasing profile in the counter-current zone (it is worth mentioning that in the counter-current the free liquor is receiving more mass than it is releasing to the chips).

The total solids content profile of the entrapped liquid can be explained by the simultaneous action of chemical reaction and mass transfer. In Fig. 11, one can see the evolution of these two factors as well as of their algebraic sum (solid line). At the beginning, both contribute positively to the solids content inside the chips and, therefore, the latter increases sharply. However, just before C_5, mass transfer contribution becomes negative (Fig. 11) leading to a clear reduction in the slope of the total solids content profile in the entrapped liquor. At C_6, since the reaction rate possesses a high maximum value, the sum of the two contributions is positive (Fig. 11) giving rise to an increasing profile of the total solids content in the entrapped liquor (Fig. 10). After this position, one can observe a short zone before the main extraction where the two contributions are symmetric, which explains the maximum of the total solids content profile in the entrapped liquor. From this point downwards, the sum of the mass transfer and chemical reaction rates is always negative, with the corresponding decrease in the profile of the total solids content in the entrapped liquid.

To evaluate the prediction capabilities of the model, industrial data was gathered from a pulp mill for a sufficiently large period of time in order to take into account the long time delays associated with the reactor and the inevitable variations of real plant data.

Table 1
Comparison between industrial and predicted values of some variables

Variable	Predicted value	Typical industrial range
T_{C_5}	144°C	143–148°C
T_{C_6}	158°C	158 – 163°C
T_{EXT}	156°C	155–164°C
T_{ITC}	149°C	145 – 152°C
T_{C_8}	117°C	110–125°C
T_{pulp}	83°C	75–85°C
E_{C_5}	20.0 g_{NaOH} dm^{-3}	14–20 g_{NaOH} dm^{-3}
E_{C_6}	18.3 g_{NaOH} dm^{-3}	11–15 g_{NaOH} dm^{-3}
E_{EXT}	5.2 g_{NaOH} dm^{-3}	4–8 g_{NaOH} dm^{-3}
E_{ITC}	9.3 g_{NaOH} dm^{-3}	7–11 g_{NaOH} dm^{-3}
E_{C_8}	7.4 g_{NaOH} dm^{-3}	4–8 g_{NaOH} dm^{-3}
$\mathscr{S}_{EXT}$	22.0%	16–19%
K_{pulp}	15.0	14.5–15.5
$cons._{pulp}$	12.0%	11.5–12.5%
η_{pulp}	53.3%	$\approx$ 52%[a]

[a]Yield of screened pulp.

The values predicted by the model as well as those characterizing the range of industrial operating conditions considered in this exercise are shown in Table 1. In general, the predictions are in good agreement with those gently provided by Portucel Industrial SA, for a given production objective with *Eucalyptus globulus*.

In what concerns effective alkali, the relative difference (between the predicted and the industrial values) at some zones is high, namely at C_5 and C_6. However, the range of variation in an industrial situation is wide and thus, the predicted values can be seen to fulfill mill's expectation. Regarding the temperature, there is a remarkable concordance between all the predicted and the industrial values. The industrial range presented, in Table 1, to T_{C_8} is much larger than the corresponding ranges to the other circulation zones. The reason for such large spread is the strong dependence of this temperature on the dilution factor used at the bottom of the digester that is difficult to tightly control for long periods of time. It is worth mentioning that the yield predicted by the model (53.3%) corresponds to the pulp at the bottom of the digester, while the industrial value refers to the pulp after screening. In summary, this is a very satisfactory capture of the behavior of the main measured variables and thus it is a promising indication of the model quality.

4. Conclusions

The steady-state operation of an industrial continuous digester with an ITC cooking strategy has been simulated by means of a model that contemplates 15 state variables in each axial position of the reactor. The model is heterogeneous and considers three different phases (solid, entrapped and free liquors). The model predicts hydrosulfide profiles in both entrapped and free liquors and includes both the temperature of the chips and of the free liquid.

Special attention was paid to the mechanical arrangements in the upper circulation zones that strongly affect the flow patterns in these areas of the reactor. The numerical strategy is based on a variable discretization scheme in order to cope with the strong discontinuities in some of the variables characterizing the free liquor. The model is able to predict the total solids content and this includes organic and inorganic materials (according to TAPPI standards and usual mill routine), which clearly distinguishes this study from previous works. In addition to the main state variables, the axial profiles of the interstitial velocities of chips and of the surrounding liquor, the Kappa number and yield are also computed. The voidage of chips is continuously updated along the digester length and the resulting incoming liquid flow is calculated according to the extent of reaction. The porosity of the moving bed of chips is determined as a function of a linear compaction profile along the axial coordinate of the digester.

The model proposed in this study is able to predict the behavior of an industrial digester with isothermal cooking under normal steady-state operation reproducing very satisfactorily the mill data processing a hardwood, *Eucalyptus globulus*. It can be easily adapted for other flow configurations, which highlights its flexibility for other studies. This is a very promising feature that anticipates its potential for optimization studies. In particular, it can be used to determine the optimal alkali distribution policies, the temperature profile and the circulation flows so that a more profitable process and a better pulp quality can be achieved.

Notation

A_d	sectional area of the digester, m^2
C_p	thermal capacity, kJ kg^{-1} K^{-1}
C_e	mass concentration of cellulose in the entrapped liquor, kg m^{-3}
C_f	mass concentration of cellulose in the free liquor, kg m^{-3}
C_s	mass fraction of cellulose based on oven dry wood, dimentionless
E	effective alkali concentration, mol dm^{-3}
f	compaction factor, dimentionless
h	liquid to wood ratio, dm^3 kg^{-1}
H_e	mass concentration of hemicellulose in the entrapped liquor, kg m^{-3}
H_f	mass concentration of hemicellulose in the free liquor, kg m^{-3}
H_s	mass fraction of hemicellulose based on oven dry wood, dimentionless
K	Kappa number, dimentionless
k_h	heat transfer coefficient, kJ min^{-1} m^{-3} K^{-1}

k_{m_i} mass transfer coefficient of species i, min^{-1}
L_e mass concentration of lignin in the entrapped liquor, kg m^{-3}
L_f mass concentration of lignin in the free liquor, kg m^{-3}
L_s mass fraction of lignin based on oven dry wood, dimentionless
Q_i volumetric flow rate of stream i, m^3 min^{-1}
Q_{m_i} mass flow rate of stream i, kg min^{-1}
r_I reaction rate of species I $(I = L, C, H, E)$, kg min^{-1} $kg_{c_{OD}}^{-1}$
$\mathscr{S}$ total solids content, %
S hydro-sulfide ion concentration, mol dm^{-3}
T temperature, K
u_i interstitial velocity of stream i $(i = s, e, f, c)$, m min^{-1}
V_{cell} volume of a reference cell of the digester, m^3
z axial coordinate of the digester, m

Greek letters
ΔH_R heat of reaction, kJ kg^{-1}
ε_c voidage of the chips, dimentionless
$\varepsilon_{c,i}$ initial voidage of the chips, dimentionless
ε_d voidage of the bed, dimentionless
ε_{pile} voidage of an outside pile of chips, dimentionless
η yield, %
$\rho_{c_{OD}}$ density of an oven dry chip, kg m^{-3}
ρ density, kg m^{-3}

Subscripts
c chips
e entrapped liquor
ext liquor extracted from the the digester
f free liquor surrounding the chips
inj liquor injected into the digester
s solid matrix of wood
soak liquor soaked by the chips due to the increase in their porosity
w white liquor

Superscripts
j number of the cell

Acknowledgements

The authors are very grateful to Dr. Paulo Barata, from Portucel Industrial, S.A. at its Setúbal mill site, for his interest in the present work and for providing relevant industrial data to validate the model. Special thanks are also due to RAIZ-Instituto de Investigação da Floresta e do Papel for enabling the use of the experimental kinetic data concerning the kraft cooking of *E. globulus*. Financial support granted by Ministry of Science and Technology under Project Praxis 3/3.2/PAPEL/2327/95 is gratefully acknowledged. The first author also wishes to thank Program Praxis for her scholarship PRAXIS/4/4.1/BD/3338.

Appendix
Reaction kinetics (Nóbrega and Castro, 1997)

Nóbrega and Castro (1997) reached experimental evidence that cellulose and hemicellulose degradation rates are distinct from each other in the pulping of *Eucalyptus globulus*. Based on this fact, they adopted a conceptual kinetic model that is similar to that proposed by Pu (1991) for softwoods, where the distinct behavior of carbohydrates is taken into account using different equations for cellulose and hemicellulose.

However, the model developed by Nóbrega and Castro (1997) is somewhat different from that of Pu (1991)

- The terms corresponding to the non-reactive substances were not considered, due to the lack of information to identify them.
- In order to reduce the number of estimated parameters, the rates of degradation of cellulose and hemicellulose are considered to be of first order relative to effective alkali and either cellulose or hemicellulose, respectively.
- The transition points are defined by lignin concentration even to carbohydrates degradation.
- A different equation for the residual phase of the degradation of hemicellulose was proposed, based on experimental evidence that hemicellulose content in this phase tends to stabilize.

A set of more than 100 cooking experiments was carried out for different reaction times, in order to follow the "history" of the process. Changing the operating conditions (alkali charge: 14, 18 and 22%; sulfidity: 17, 25 and 40%; temperature: 150, 160 and 170°C) it was possible to obtain the experimental data which characterizes the kinetics of the reactions. These data were then used in an optimization procedure to fit the model (minimization of the weighted sum of the square errors between observations and model predictions).

In the kinetic separations, L, C and H correspond to the solid phase while E and S refer to the entrapped liquor phase

Period	Kinetic rate
Initial	$\frac{dL}{dt} = -e^{6.12-(4307.69/T)}L$
$(L > 18{,}5\%)$	$\frac{dC}{dt} = -e^{4.16-(3708/T)}E\,C$
	$\frac{dH}{dt} = -e^{11.62-(6454.6/T)}E\,H$

Bulk

$$\frac{dL}{dt} = -(e^{35.19-(16100/T)}E + e^{29.23-(14400/T)} \times E^{0.03}S^{0.87})L$$

$(2.0\% < L < 18.5\%)$

$$\frac{dC}{dt} = -e^{27.28-(14256.9)/T}E\,C$$

$$\frac{dH}{dt} = -e^{18.25-(9379.9/T)}E\,H$$

Residual

$$\frac{dL}{dt} = -e^{19.64-(9800)/T}E^{1.7}L$$

$(L < 2.0\%)$

$$\frac{dC}{dt} = -e^{27.28-(14256.9/T)}E\,C$$

$$\frac{dH}{dt} = -e^{5.32-(7443.4/T)}E\,H$$

Initial, bulk, residual

$$\frac{dE}{dt} = \frac{1}{h}\left(1.01\frac{dL}{dt} + 8.199\left(\frac{dC}{dt} + \frac{dH}{dt}\right)\right)$$

References

Christensen, T., Albright, C. F., & Williams, T. J. (1982). *A mathematical model of the kraft pulping process.* Technical Report 129, Purdue University, West Lafayette, USA.

Giudici, R., & Park, S. W. (1996). Kinetic model for kraft pulping of hardwood. *Industrial and Engineering Chemistry Research*, *35*(3), 856–863.

Grace, T. M., & Malcolm, E. W. (Eds.). (1989). Pulp and paper manufacture-alkaline pulping, vol. 5 (3rd ed.). Technical Section of the Canadian Pulp & Paper Association, Montreal, Canada.

Gustafson, R. R., Shelder, C. A., McKean, W. T., & Finlayson, B. A. (1983). Theoretical model of the kraft pulping process. *Industrial and Engineering Chemistry Process Design and Development*, *22*(1), 87–96.

Härkönen, E. J. (1987). A mathematical model for two-phase flow in a continuous digester. *Tappi Journal*, *70*(12), 122–126.

Johnsson, L. (1970). *Mathematical models of the kraft cooking process.* Technical Report 11, Department of Control Engineering, Chalmers University of Technology, Gothenburg, Sweden.

Magalhães, S. L. F., Bastos, M. J. T. G., Martins, A. J. R., Simões, R. M. S., & Castro, J. A. A. M. (1998). Mass transfer of inorganic chemicals in wood chips during the impregnation stage of kraft cooking. In *CHEMPOR-98 seventh international chemical engineering conference*, Lisbon, IST-UTL, pp. 1271–1278.

Michelsen, F. (1995). A dynamic mechanistic model and model-based analysis of a continuous Kamyr digester. Ph.D. Thesis, The Norwegian Institute of Technology, Trondheim, Norway.

Nóbrega, A., & Castro, J. (1997). *Modelo cinético — cozimento do Eucalyptus globulus*. Internal Report, RAIZ-Instituto de Investigação da Floresta e Papel, Eixo, Portugal.

Pu, Q. (1991). Theoretical and experimental studies of the RDH (Rapid Displacement Heating) pulping process. Ph.D. Thesis, University of Washington.

Santos, A., Rodríguez, F., Gilarranz, M., Moreno, D., & García-Ochoa, F. (1997). Kinetic modeling of kraft delignification of Eucalyptus globulus. *Industrial and Engineering Chemical Research*, *36*(10), 4114–4125.

Smith, C. C., & Williams, T. J. (1974). *Mathematical modeling, simulation and control of the operation of a kamyr digester for kraft process.* Technical Report 64, Purdue University, West Lafayette, USA.

Vroom, K. E. (1957). The "H" factor: A means of expressing cooking times and temperatures as a single variable. *Pulp and Paper Canada*, *58*(3), 228–231.

Wisnewski, P. A., & Doyle III, F. J. (1996). A reduced model approach to estimation and control of a kamyr digester. *Computers and Chemical Engineering*, *20*(Suppl.), S1053–S1058.

Wisnewski, P. A., Doyle III, F. J., & Kayihan, F. (1997). Fundamental continuous-pulp-digester model for simulation and control. *A.I.C.h.E. Journal*, *43*(12), 3175–3192.